

DNA condensation for gene therapy as monitored by atomic force microscopy

Helen G. Hansma*, Roxana Golan, Wan Hsieh, Charles P. Lollo¹, Patricia Mullen-Ley¹ and Deborah Kwoh¹

Department of Physics, University of California, Santa Barbara, CA 93106, USA and ¹The Immune Response Corporation, 5935 Darwin Court, Carlsbad, CA 92008, USA

Received December 15, 1997; Revised and Accepted March 25, 1998

ABSTRACT

The atomic force microscope (AFM) was used to assay the extent of DNA condensation in ~100 different complexes of DNA with polylysine (PL) or PL covalently attached to the glycoproteins asialoorosomuroid (AsOR) or orosomuroid (OR). The best condensation of DNA was obtained with 10 kDa PL covalently attached to AsOR, at a lysine:nucleotide (Lys:nt) ratio of 5:1 or higher. These conditions produce large numbers of toroids and short rods with contour lengths of 300–400 nm. Some DNA condensation into shortened thickened structures was seen with 10 kDa PL attached to AsOR at Lys:nt ratios of 1.6:1 and 3:1. Some DNA condensation was also seen with 4 kDa PL at Lys:nt ratios of 3:1 and higher. Little DNA condensation was seen with PL alone or with PL covalently attached to OR at Lys:nt ratios up to 6:1. AsOR–PL enhanced gene expression in the mouse liver ~10- to 50-fold as compared with PL alone.

INTRODUCTION

Atomic force microscopy (AFM, also known as SFM) is becoming increasingly useful for biological research (1–6). AFM has been used here to image complexes of DNA designed to target the asialoglycoprotein receptor of liver cells (7–10).

Inserting genes into cells has been a goal of medical research for many years. The ways of doing this generally involve compacting the DNA and packaging it with something that will facilitate its uptake into cells. Receptor-mediated gene therapy (11–13) is less popular at present than viral-mediated gene therapy, which has been more successful at productively introducing genes into cells. New questions about the safety of viral vectors (14) provide an impetus for continuing research on receptor-mediated DNA delivery, which can be used to introduce longer DNA sequences (12) and can be targeted to specific cell types.

AFM has potential value for assaying DNA condensation for any mode of gene therapy. DNA condensation with proteins is easily assayed by AFM in air or dry gas, as demonstrated here and elsewhere (15). DNA condensation with liposomes (16) has been

assayed by EM in vacuum (17), but it could also be assayed by AFM in aqueous solution, which might be preferable, since liposomes are generally unstable in air.

MATERIALS AND METHODS

Substrates

Mica. Discs of mica (Ruby Muscovite Mica; New York Mica Co., New York, NY) were glued with 2-Ton epoxy resin (Devcon Corporation, Wood Dale, IL) to steel discs that had a transmission electron microscopy locator grid (Microscopy Sciences, Fort Washington, PA) glued to the center (18). Mica discs were cleaved with adhesive tape immediately before use.

Samples

DNA–polylysine (PL) complexes were prepared in water, in neutral saline (0.15 M NaCl, pH ~7) and in alkaline saline (0.15 M NaCl, 0.002 M NaOH, pH ~11) as specified below. The DNA concentration was 10 ng/μl for all complexes.

Two DNA plasmids were used: pCMV luciferase (19) (6832 bp) for AFM images in all figures except Figures 2C and 8; pCY2 (9700 bp) for Figures 2C and 8.

Polylysines of three different sizes were used: 4 (Lys₂₀), 10 (Lys₅₀) and 26 (Lys₁₂₀) kDa. The numerical subscripts, e.g. Lys₂₀, are the calculated mean number of lysine residues for molecules of polylysine hydrobromide (Sigma, St Louis, MO) with the specified mean molecular weights.

Asialoorosomuroid (AsOR)–PL conjugates were prepared by carbodiimide coupling (20).

PL:DNA ratios are lysine residues:DNA nucleotides (Lys:nt). The complexes listed below were prepared at the following Lys:nt ratios: 0.2:1, 0.3:1, 0.5:1, 0.6:1, 1.6:1, 3:1, 5:1 and 6:1. (i) 4 kDa PL–AsOR + DNA in neutral saline or alkaline saline; (ii) 4 kDa PL–orosomuroid (OR) + DNA in neutral saline or alkaline saline; (iii) 4 kDa PL + DNA in neutral saline, alkaline saline or water; (iv) 10 kDa PL–AsOR + DNA in neutral saline or alkaline saline; (v) 10 kDa PL–AsOR + DNA in water; (vi) 26 kDa PL–AsOR + DNA in water. 26 kDa PL–AsOR + DNA at a Lys:nt ratio of 3:1 was supplied in neutral saline.

*To whom correspondence should be addressed. Tel: +1 805 893 3881; Fax: +1 805 893 8315; Email: hhansma@physics.ucsb.edu

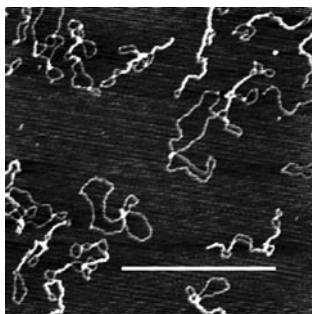


Figure 1. Bare plasmid DNA (6832 bp) imaged in the AFM in air. The DNA was dialyzed against HEPES, Mg^{2+} as described in Materials and Methods. The DNA did not bind to mica in either neutral saline or alkaline saline. The image is $2 \times 2 \mu\text{m}$. Scale bar $1 \mu\text{m}$.

Samples of spermine + DNA with 10, 100 or 500 mM spermine were prepared in 45 mM Tris, 150 mM NaCl, pH 7.2.

Sample preparation

Samples in neutral saline. Samples were prepared by placing $2 \mu\text{l}$ solution on a freshly cleaved mica surface. After 60 s they were rinsed with 1–2 ml H_2O , dried with a stream of filtered compressed air and further dried in a desiccator over P_2O_5 .

Samples in alkaline saline. Samples were prepared by placing $1 \mu\text{l}$ solution on a freshly cleaved mica surface. They were immediately rinsed with H_2O , dried with a stream of compressed air and further dried in a desiccator over P_2O_5 .

The different conditions for preparing samples in neutral saline and alkaline saline were chosen because these conditions gave good densities of DNA complexes on the mica surface, i.e. DNA complexes in alkaline saline bound to mica more readily than those in neutral saline.

Samples in water. Samples were prepared by placing 1–5 μl solution on a freshly cleaved mica surface. They were dried with a stream of compressed air either immediately or after sitting for 1–3 min. A few samples were also prepared by the method of Wolfert and Seymour (21): 5 μl solution on mica was rinsed after 5 min with three rinses of 100 μl water/rinse and dried by evaporation at room temperature.

Some samples in water were diluted with or dialyzed against 40 mM HEPES, 10 mM $MgCl_2$, pH 7.6, (18) as specified in Figures 1 and 3.

AFM imaging

Tapping mode AFM in air was done with a MultiMode AFM and Nanoscope III (Digital Instruments, Santa Barbara, CA). Bungee cords were used for vibration isolation (22). The D scanner was used for all samples. The D scanner was accurate to 8% in the xy directions, calibrated using a known grating. Standard 125 μm silicon cantilevers were obtained from Digital Instruments.

Images were processed by flattening to remove the background slope. Two-dimensional Fourier filtering was used to reduce the periodic noise in Figure 1. Molecular lengths were calculated by summing the fragment lengths measured using the cursor command in the Nanoscope software (v.3.12).

Assaying gene incorporation *in vivo*

Balb/c mice (Charles River Laboratories, Wilmington, MA) were injected in the tail vein with DNA–PL complexes, as described in Table 1. Excised livers were rinsed with phosphate-buffered saline, weighed, lysed (in 100 mM potassium phosphate, pH 7.8, 0.2% Triton X-100), homogenized and centrifuged. The clear liquid between the top fat layer and the cell pellet was collected. Luciferase activity was assayed in 5–10 μl aliquots of this clear liquid layer (23). After subtraction of the background, luciferase activity was converted to pg protein as calculated from the standard curves based on purified luciferase protein standards.

Table 1. AsOR enhances *in vivo* gene expression in liver

DNA complexed with:	Gene expression: pg luciferase/g liver
4 kDa PL	94 ± 16
10 kDa PL	705 ± 440
4 kDa PL-AsOR	7860 ± 2600
10 kDa PL-AsOR	6090 ± 4040

Three mice per group were tail-vein injected with 1 ml of DNA complex in 0.15 M NaCl. All complexes had a Lys:nt ratio of 1:1 and a DNA concentration of 10 $\mu\text{g}/\text{ml}$. Livers were harvested 48 h post-injection and assayed for luciferase protein. Data are mean \pm SEM.

Purified luciferase enzyme can be quantitated accurately after dilution into cell extract. This indicates that the cell extract or ‘clear liquid layer’ does not interfere with the luciferase assay.

RESULTS

Polylysine–DNA complexes

In saline. PL condensed DNA poorly or not at all in neutral saline or alkaline saline, even at Lys:nt ratios of 3:1 and 6:1. The AFM images in Figure 2 are arranged in order of increasing Lys:nt ratios from 0.3:1 to 6:1. Both longer and shorter PL molecules gave similar results: 26 kDa PL was used in Figure 2C and 4 kDa PL was used in Figure 2A, B and D. The length of the DNA condensed with PL was the same as the length of the bare DNA molecules, $\sim 2 \mu\text{m}$ (Figs 1 and 2A and B).

In some samples most of the complexes were highly oriented (see for example Fig. 2B and C). There was no correlation between the degree of orientation and Lys:nt ratio; samples with linearly oriented complexes and samples with randomly oriented complexes were found at both low and high Lys:nt ratios. In fact, the two images of randomly oriented complexes (Fig. 2A and D) are the samples with the lowest and the highest Lys:nt ratios. The degree of orientation in these samples is probably proportional to the force of the compressed air that was used to dry the sample.

In water. Several PL–DNA complexes were also prepared in water instead of saline. Samples in water gave better results with EM (not shown), but samples in physiological saline are more relevant for comparison with *in vivo* results.

Samples in water were dried in different ways. The morphologies of the complexes varied according to the method used for drying them. Samples dried with compressed air showed partially condensed complexes (Fig. 3A and B). Samples dried by evaporation in ambient air showed blobs of variable size with, in some cases, short loops projecting from them.

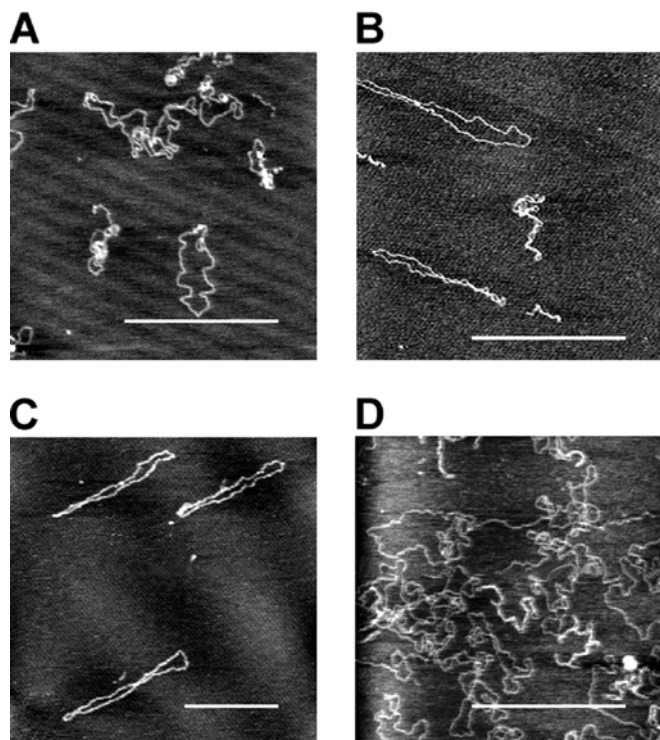


Figure 2. Complexes of DNA + PL at increasing Lys:nt ratios, imaged by AFM in air. (A) Lys:nt 0.5:1, alkaline saline; (B) Lys:nt 2:1, neutral saline; (C) Lys:nt 3:1, neutral saline; (D) Lys:nt 6:1, alkaline saline. (A, B and D) 6832 bp plasmid DNA, 4 kDa PL, images $2 \times 2 \mu\text{m}$; (C) 9700 bp plasmid DNA, 26 kDa PL, image $3.5 \times 3.5 \mu\text{m}$. Scale bars $1 \mu\text{m}$.

Samples dried by evaporation may have artifactual aggregation induced by the receding meniscus during drying. Samples dried with compressed air may have artifactual decreases in condensation and aggregation caused by the drying method. Drying with compressed air will disrupt weakly condensed and aggregated molecules and only strong condensation and aggregation will be observed after drying with compressed air. Except for the samples in Figure 3C, all the samples in Figures 1–9 were dried with compressed air. Therefore, differences among these samples are not due to differences in the drying method.

When PL–DNA in water was dried with compressed air, binding to mica was so poor that no PL–DNA complexes were seen by AFM in most of the samples. In the few samples in which complexes were seen most of the complexes were somewhat more condensed than in saline solutions (Fig. 2 versus Fig. 3A and B). The degree of condensation was comparable for DNA complexes with 10 kDa PL (Fig. 3A) and 4 kDa PL (Fig. 3B).

The samples dried by evaporation in ambient air had complexes that were similar to those obtained by Wolfert and Seymour (21), who prepared their samples by the same method. In addition, there were strands of DNA (Fig. 3C, arrows), especially around the edges of blobs, probably because tapping AFM generally gives better resolution on biomolecules (24,25) than the contact AFM as used by Wolfert and Seymour.

Some of the samples in water were diluted 5- to 10-fold with a HEPES, Mg^{2+} solution. This greatly increased binding to mica and produced daisy-shaped aggregates (Fig. 3D). Similar

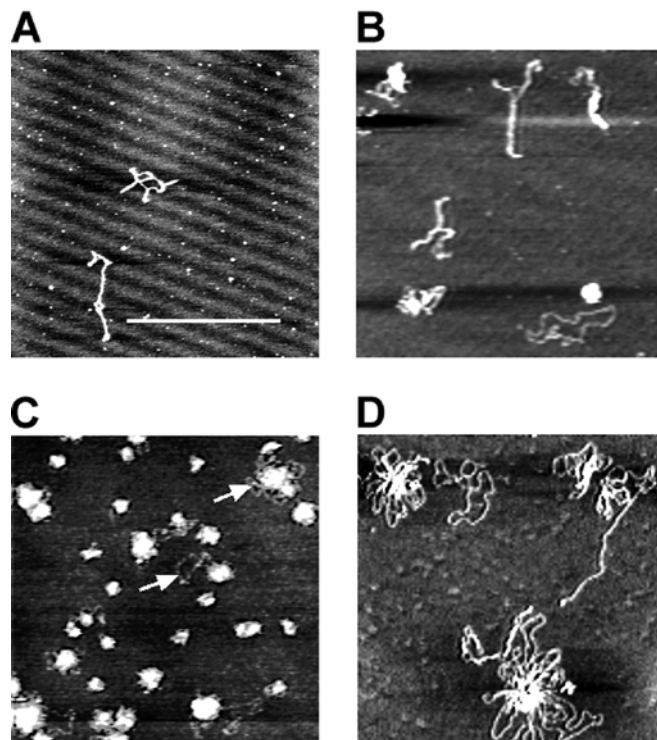


Figure 3. Complexes of DNA + PL in water (A–C) and HEPES, Mg^{2+} (D), imaged by AFM in air. (A) 10 kDa PL, Lys:nt 0.6:1; (B) 4 kDa PL, Lys:nt 0.6:1; (C) 10 kDa PL, Lys:nt 2:1 (sample prepared as in 21); (D) 4 kDa PL, Lys:nt 0.5:1. Images are $2 \times 2 \mu\text{m}$. Scale bar $1 \mu\text{m}$.

conformations of DNA have been seen by EM of DNA spread at low ionic strength (26).

Orosomucoïd–polylysine–DNA complexes

OR–PL was also poor at condensing DNA (Fig. 4). As with the PL–DNA complexes, there were no clear differences between complexes in neutral and alkaline saline. These complexes typically appeared as circles or diffuse aggregates.

Particulate backgrounds were often seen with OR–PL complexes (see for example Fig. 4B), while the backgrounds were generally quite clean with PL complexes (Figs 2 and 3). These particles may be OR–PL, which was present in solution in these samples but not in the PL samples. Alternatively, it is possible that OR–PL binds to mica better than PL and that this is the cause of the particulate backgrounds in Figure 4.

Asialorosomucoïd–polylysine–DNA complexes

AsOR–PL condensed DNA much better than PL alone or OR–PL. The most condensed complexes of AsOR–PL–DNA were toroids and short rods with contour lengths of 300–400 nm (Fig. 5). These complexes were seen with 10 kDa PL at Lys:nt ratios of 5:1 and 6:1. Complexes stored in solution at 4°C for 8 months still gave AFM images comparable with those shown in Figure 5.

DNA condensation with AsOR–PL was much greater with 10 (Figs 5 and 6) than with 4 kDa PL (Fig. 7). With 10 kDa PL toroids

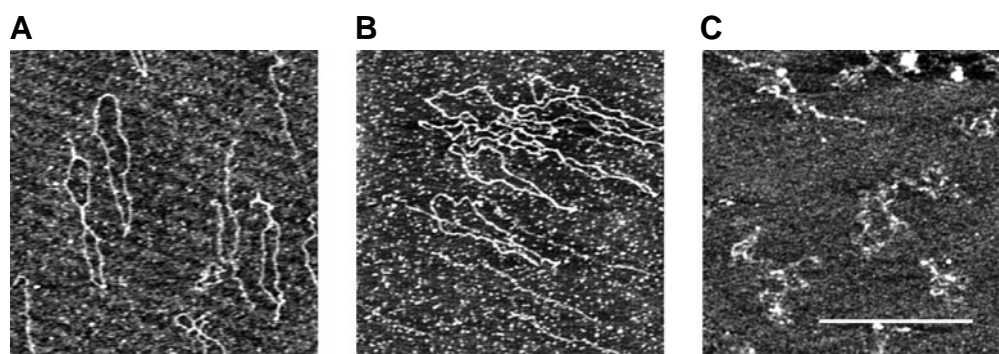


Figure 4. Complexes of DNA + 4 kDa PL-OR, imaged by AFM in air. (A) Lys:nt 0.3:1, neutral saline; (B) Lys:nt 0.5:1, alkaline saline; (C) Lys:nt 6:1, neutral saline. Images are $2 \times 2 \mu\text{m}$. Scale bar $1 \mu\text{m}$.

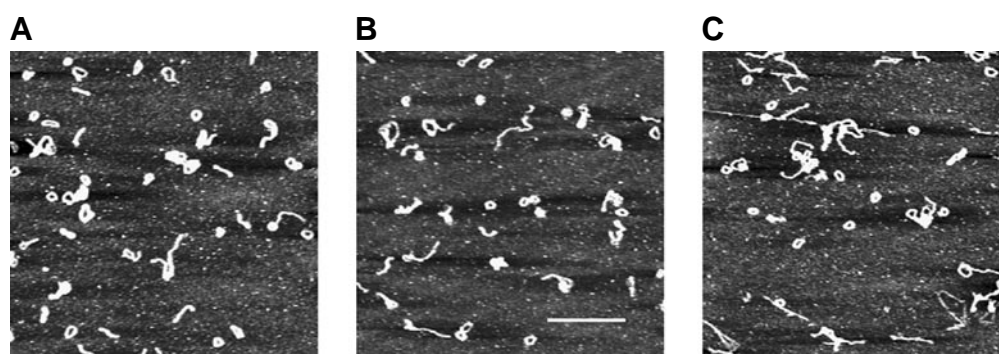


Figure 5. Complexes of DNA + 10 kDa PL-AsOR with the best condensation of DNA were seen at Lys:nt ratios of 5:1 (A and B) and 6:1 (C). Samples were applied to mica in neutral saline (A and C) or alkaline saline (B) and were imaged by AFM in air. Images are $4 \times 4 \mu\text{m}$. Scale bar $1 \mu\text{m}$.

were seen at Lys:nt ratios of 2:1 and higher (Figs 5 and 6C and F), while with 4 kDa PL toroids were seen only at a Lys:nt ratio of 6:1.

One complex of DNA with 26 kDa PL-AsOR at a 3:1 Lys:nt ratio (Fig. 8) showed condensed molecules aggregated with other condensed molecules to form long thick branched and looped structures.

The densities of complexes on the surface were independent of the Lys:nt ratio. Therefore, the different complexes appear to have similar affinities for the mica surface and the different morphologies of different complexes should reflect actual differences in solution rather than artifactual differences due to selective binding of different subsets of molecules. As with OR-PL-DNA complexes, there were often particles on the mica surface with many of the samples of AsOR-PL-DNA.

The densities of complexes on the surface depended on the pH of the saline solution. DNA complexes adsorbed to mica better from alkaline saline than from neutral saline, as evidenced by a greater density of complexes on the mica surface with alkaline saline under identical conditions for sample preparation. To increase the adsorption of complexes in neutral saline we used larger volumes of sample and allowed them to sit longer on the mica before rinsing, as described in Materials and Methods. There was no consistent difference in appearance between the samples in neutral saline that remained on the mica before rinsing and the samples in alkaline saline that were rinsed immediately (Fig. 6A-C versus D-F).

Spermine-DNA complexes

In the presence of spermine, DNA molecules and clusters of molecules showed nodes of condensation. In 10 mM spermine these nodes were seen within individual DNA molecules (Fig. 9A), while in 500 mM spermine several molecules were clustered together at the nodes, which were in some cases quite dense (Fig. 9B). The effect of drying on these structures was not investigated, but weakly condensed/aggregated DNA may have been dispersed by drying with compressed air.

Heights of complexes

Plasmid DNA molecules had apparent heights of $0.28 \pm 0.05 \text{ nm}$, which is similar to heights previously measured with AFM (27). The AFM tip often compresses biomaterials during imaging. Similar heights were measured for $2 \mu\text{m}$ long PL-DNA complexes.

As the DNA became more condensed, its height increased. Toroids and short rods (Fig. 5) had measured heights of 3–4 nm.

Gene expression *in vivo*

At 1:1 Lys:nt AsOR-PL was much better than PL alone for producing DNA complexes whose luciferase genes could be expressed in mouse liver (Table 1). Luciferase gene expression was similar for 4 and 10 kDa PL-AsOR. Luciferase gene

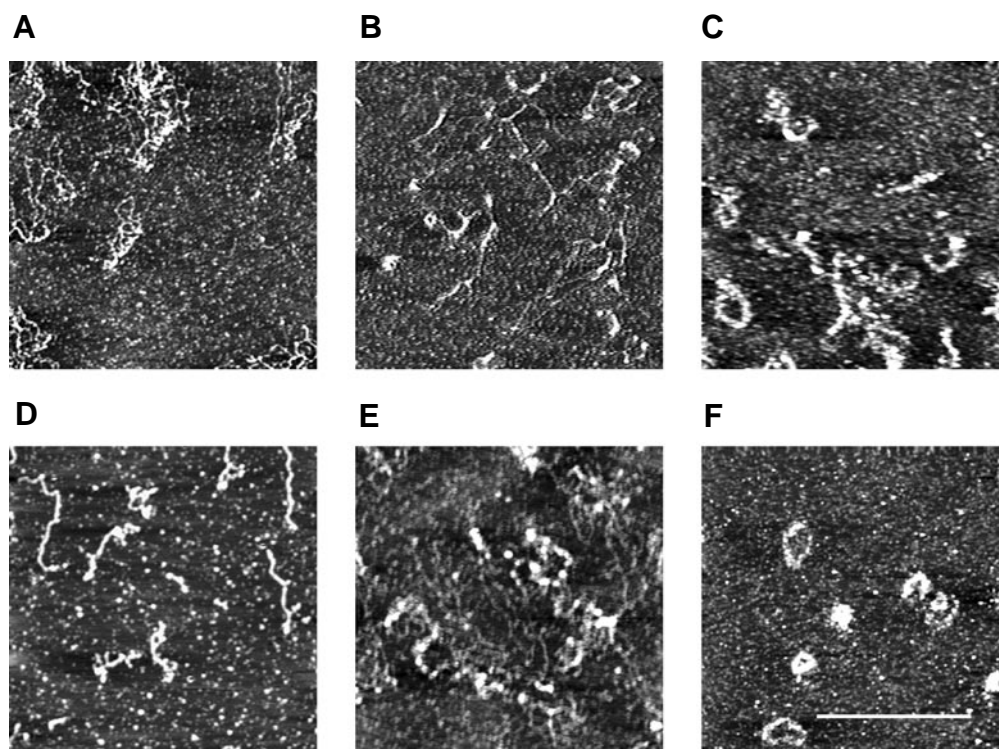


Figure 6. Complexes of DNA + 10 kDa PL-AsOR in neutral saline (A-C) or alkaline saline (D-F), imaged with the AFM in air. Ratios of Lys:nt are 0.5:1 (A and D), 0.6:1 (B and E) and 2:1 (C and F). Images are $2 \times 2 \mu\text{m}$. Scale bar $1 \mu\text{m}$.

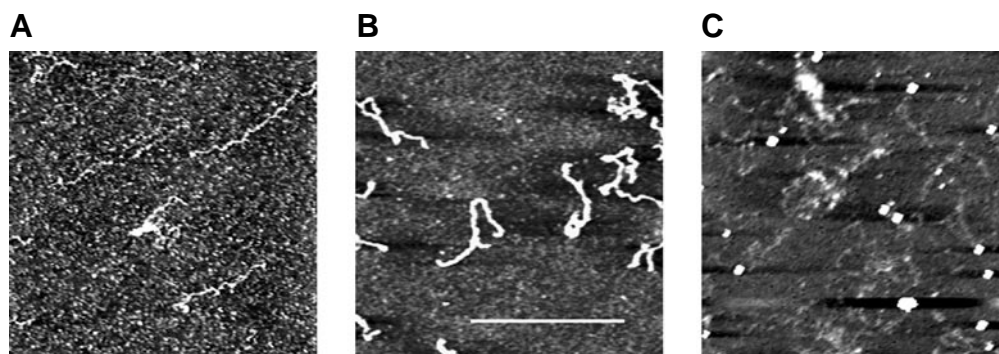


Figure 7. Complexes of DNA + 4 kDa PL-AsOR, imaged with the AFM in air. (A) 0.6:1 Lys:nt ratio, alkaline saline; (B) 3:1 Lys:nt, neutral saline; (C) 5:1 Lys:nt, alkaline saline. Images are $2 \times 2 \mu\text{m}$. Scale bar $1 \mu\text{m}$.

expression was significantly higher for 10 than for 4 kDa PL in the absence of AsOR. None of the complexes tested *in vivo* showed a high degree of condensation by AFM.

DISCUSSION

The two objectives of this research were: (i) to develop AFM into a useful tool for assaying DNA condensation for gene therapy and other applications; and (ii) to find the conditions that give the most complete condensation of DNA with AsOR. Good condensation of

DNA correlates strongly with receptor-mediated DNA uptake, at least for the transferrin receptor (28).

The complexes shown here are well-condensed complexes, as condensation is present even after rinsing and drying with compressed air.

Several conclusions can be drawn from this research. First, good DNA condensation was obtained only with AsOR-PL (Fig. 5). Neither PL nor OR-PL condensed the DNA into compact particles even at ratios of up to 6:1 Lys:nt (Figs 2-4). Second, 10 kDa PL-AsOR condensed the DNA much better than 4 kDa PL-AsOR (Figs 5 and 6 versus 7). Third, with 10 kDa PL-AsOR, condensation

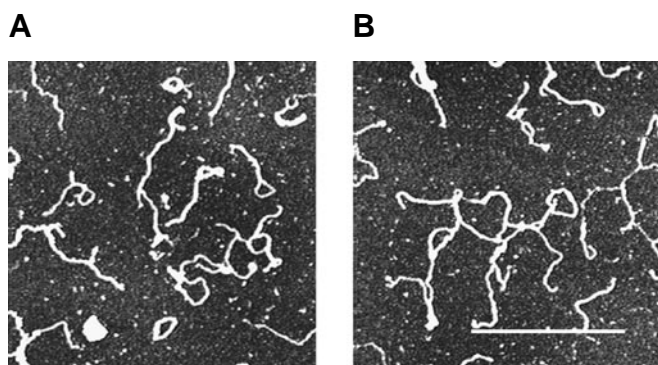


Figure 8. Complexes of 9700 bp plasmid DNA + 26 kDa PL-AsOR at a 3:1 Lys:nt ratio in neutral saline. AFM imaging in air. Images are $2 \times 2 \mu\text{m}$. Scale bar $1 \mu\text{m}$.

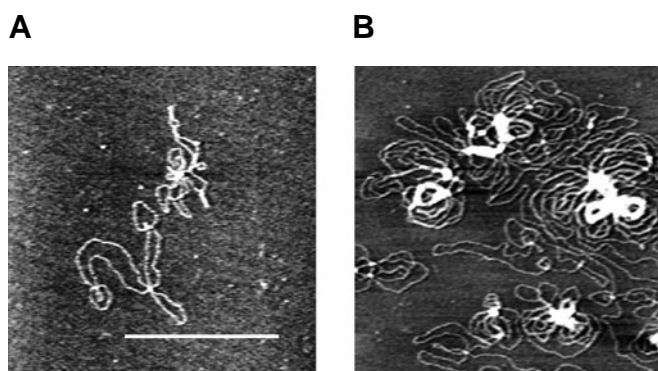


Figure 9. Complexes of DNA with (A) 10 mM and (B) 500 mM spermine. Images are $2 \times 2 \mu\text{m}$. Scale bar $1 \mu\text{m}$.

was greatest with Lys:nt ratios of 5:1 or 6:1, when many small toroids and short rods were seen. Toroids were also seen with 10 kDa PL-AsOR at Lys:nt ratios as low as 2:1 (Fig. 6C and F), but the toroids were less compact and more aggregation was seen.

With 26 kDa PL-AsOR there was intermolecular aggregation of DNA at a 3:1 Lys:nt ratio (Fig. 8), while with 10 kDa PL-AsOR there were mostly isolated toroids at this Lys:nt ratio (Figs 5 and 6). We do not have data for 26 kDa PL-AsOR at lower Lys:nt ratios.

AFM is convenient and fast for these investigations. After the methods for sample preparation have been developed for a specific system, DNA samples in solution can be applied to mica, dried and imaged by AFM under dry gas in ~ 15 min. Sample changing usually requires < 5 min. Thus we typically imaged these samples at a rate of 2–5/h.

Although AFM can image samples in aqueous solution, it is usually easier to image samples in air. Imaging in air also uses a smaller quantity of sample. Sample volumes as small as $0.2 \mu\text{l}$ can be pipetted onto mica above an EM locator grid for AFM in air (25). Sample volumes of $35 \mu\text{l}$ or more are used for AFM in fluid. Both in air and in fluid AFM can image only the molecules that are at the surface. Therefore, AFM in air is generally used for routine screening of large numbers of samples.

It is also easier with AFM in air to adsorb the complexes to the surface strongly enough for stable imaging. For example, Dunlap *et al.* (29) used bare mica for AFM of polycation–DNA in air, but they needed polyornithine-coated mica to image the same complexes in fluid. AFM in fluid is needed for imaging motion or processes (30,31) or for imaging samples such as liposomes (32), whose gross structures are dependent upon being in solution.

Structures and conformations of DNA–protein complexes may, however, be altered by drying. DNA complexes with *Escherichia coli* RNA polymerase appear similar in air and in fluid, but DNA complexes with polycations may be more sensitive to drying artifacts. We show here that the method of drying affects the appearance of DNA–PL complexes (Fig. 3A–C).

Complexes of DNA with other polycations have been imaged by AFM in air and in fluid (15,29). The structure of DNA–protamine complexes in air depended on the sample preparation method (15). When the DNA and protamine were mixed before applying them to the mica DNA networks with small circular regions appeared on the mica. When DNA was loosely adsorbed to mica before adding protamine, condensed toroids appeared in the DNA network.

With the polycations lipospermine or polyethylenimine (PEI) DNA was condensed at sub-saturating concentrations of polycation and aggregated at higher concentrations of polycation, as observed by AFM in aqueous fluid (29). Dried complexes of DNA with PEI showed a different morphology, but they were also deposited onto a different surface, which might account for the differences.

DNA complexes designed for receptor-mediated gene therapy have also been imaged by EM (7,10,28). EM of a DNA analog condensed with AsOR showed 50–150 nm toroids (7). EM of DNA condensed with transferrin–PL showed toroids, diffuse aggregates and less condensed structures, depending on the ratios of DNA to transferrin to PL (28).

Complexes of DNA with galactosylated PL were prepared by gradually neutralizing the DNA with galactosylated PL and then raising the ionic strength to solubilize the complexes progressively into condensed structures and relaxed circles, as observed by EM. Transfection activity was nil for aggregated complexes and showed tissue-dependent differences in activity for condensed and relaxed complexes (10). With AFM we found that complexes of DNA with lactosylated PL (3:1 Lys:nt) were loosely aggregated in isotonic saline, rather like the complexes in Figure 2D, and they were dissociated into individual relaxed circles by diluting them 5-fold with water (data not shown).

Toroids have been seen by EM of DNA condensed with PL (33) and with spermidine (34). Toroids were not seen with AFM with either PL or spermine, although the nodes seen in 500 mM spermine were quite dense. Very high concentrations of PL (300–3000 Lys:nt) were used to condense DNA into toroids and rods (33). We have not looked at such high Lys:nt ratios by AFM. Spermidine–DNA toroids were found at low ionic strength (34), while aggregation of spermidine–DNA occurred in isotonic saline (35), which was also used for the spermine–DNA complexes of Figure 9.

Investigating the mechanism of DNA condensation is important not only for gene delivery, but also for understanding natural biological processes that require DNA condensation, such as viral replication and cell division. This has recently been reviewed (36). An important direction for future AFM research on DNA condensation is to compare the morphologies of DNA complexes

in air and in aqueous solution. It may also be possible to observe the process of DNA condensation by AFM.

ACKNOWLEDGEMENTS

We thank C.R.Ill and Alison Phillips for providing DNA-PL samples, Scott Hansma for software development and Christine Chen for expert technical assistance. This work was supported by NSF grants MCB9604566 (H.G.H., W.H. and R.G.), DMR9632716 (R.G.), and Digital Instruments.

REFERENCES

- Hansma, H.G., Kim, K.J., Laney, D.E., Garcia, R.A., Argaman, M. and Parsons, S.M. (1997) *J. Struct. Biol.*, **119**, 99–108.
- Mueller, D.J., Schoenenberger, C.A., Schabert, F. and Engel, A. (1997) *J. Struct. Biol.*, **119**, 149–157.
- Shao, Z., Mou, J., Czajkowsky, D.M., Yang, J. and Yuan, J.-Y. (1996) *Adv. Phys.*, **45**, 1–86.
- Henderson, E. (1994) *Prog. Surface Sci.*, **46**, 39–60.
- Hansma, H.G. and Hoh, J. (1994) *Annu. Rev. Biophys. Biomol. Struct.*, **23**, 115–139.
- Bustamante, C., Erie, D.A. and Keller, D. (1994) *Curr. Opin. Struct. Biol.*, **4**, 750–760.
- Bunnell, B.A., Askari, F.K. and Wilson, J.M. (1992) *Somat. Cell Mol. Genet.*, **18**, 559–569.
- Wilson, J.M., Grossman, M., Wu, C.H., Chowdhury, N.R., Wu, G.Y. and Chowdhury, J.R. (1992) *J. Biol. Chem.*, **267**, 963–967.
- Ferkol, T., Lindberg, G.L., Chen, J., Perales, J.C., Crawford, D.R., Ratnoff, O.D. and Hanson, R.W. (1993) *FASEB J.*, **7**, 1081–1091.
- Perales, J.C., Grossmann, G.A., Molas, M., Liu, G., Ferkol, T., Harpst, J., Oda, H. and Hanson, R.W. (1997) *J. Biol. Chem.*, **272**, 7398–7407.
- Christiano, R.J. and Curiel, D.T. (1996) *Cancer Gene Ther.*, **3**, 49–57.
- Phillips, S.C. (1995) *Biologicals*, **23**, 13–16.
- Perales, J.C., Ferkol, T., Molas, M. and Hanson, R.W. (1994) *Eur. J. Biochem.*, **226**, 255–66.
- Marshall, E. (1995) *Science*, **269**, 1050–1055.
- Allen, M.J., Bradbury, E.M. and Balhorn, R. (1997) *Nucleic Acids Res.*, **25**, 2221–2226.
- Gao, X. and Huang, L. (1996) *Biochemistry*, **35**, 1027–1036.
- Dzau, V.J., Mann, M.J., Morishita, R. and Kaneda, Y. (1996) *Proc. Natl. Acad. Sci. USA*, **93**, 11421–11425.
- Bezanilla, M., Manne, S., Laney, D.E., Lyubchenko, Y.L. and Hansma, H.G. (1995) *Langmuir*, **11**, 655–659.
- Merwin, J.R., Noell, G.S., Thomas, W.L., Chiou, H.C., DeRome, M.E., McKee, T.D., Spitalny, G.L. and Findeis, M.A. (1994) *Bioconjugate Chem.*, **5**, 612–20.
- McKee, T.D., DeRome, M.E., Wu, G.Y. and Findeis, M.A. (1994) *Bioconjugate Chem.*, **5**, 306–311.
- Wolfert, M.A. and Seymour, L.W. (1996) *Gene Ther.*, **3**, 269–273.
- Hansma, H.G., Bezanilla, M., Laney, D.L., Sinsheimer, R.L. and Hansma, P.K. (1995) *Biophys. J.*, **68**, 1672–1677.
- Hickman, M.A., Malone, R.W., Lehmann-Bruinsma, K., Sih, T.R., Knoell, D., Szoka, F.C., Walzem, R., Carlson, D.M. and Powell, J.S. (1994) *Hum. Gene Ther.*, **5**, 1477–1483.
- Hansma, H.G., Sinsheimer, R.L., Groppe, J., Bruice, T.C., Elings, V., Gurley, G., Bezanilla, M., Mastrangelo, I.A., Hough, P.V.C. and Hansma, P.K. (1993) *Scanning*, **15**, 296–299.
- Hansma, H.G., Browne, K.A., Bezanilla, M. and Bruice, T.C. (1994) *Biochemistry*, **33**, 8436–8441.
- Inman, R.B. (1967) *J. Mol. Biol.*, **25**, 209–216.
- Hansma, H.G., Revenko, I., Kim, K. and Laney, D.E. (1996) *Nucleic Acids Res.*, **24**, 713–720.
- Wagner, E., Cotten, M., Foisner, R. and Birnstiel, M.L. (1991) *Proc. Natl. Acad. Sci. USA*, **88**, 4255–4259.
- Dunlap, D.D., Maggi, A., Soria, M.R. and Monaco, L. (1997) *Nucleic Acids Res.*, **25**, 3095–3101.
- Kasas, S., Thomson, N.H., Smith, B.L., Hansma, H.G., Zhu, X., Guthold, M., Bustamante, C., Kool, E.T., Kashlev, M. and Hansma, P.K. (1997) *Biochemistry*, **36**, 461–468.
- Bezanilla, M., Drake, B., Nudler, E., Kashlev, M., Hansma, P.K. and Hansma, H.G. (1994) *Biophys. J.*, **67**, 2454–2459.
- Muller, D.J., Amrein, M. and Engel, A. (1997) *J. Struct. Biol.*, **119**, 172–188.
- Laemmli, U.K. (1975) *Biochemistry*, **72**, 4288–4292.
- Chattoraj, D. K. and Gosule, L.C. (1978) *J. Mol. Biol.*, **121**, 327–337.
- Gosule, L.C. and Schellman, J.A. (1978) *J. Mol. Biol.*, **121**, 311–326.
- Bloomfield, V.A. (1996) *Curr. Opin. Struct. Biol.*, **6**, 334–341.